tvst

Article

The Clinical Application of Polarization Pattern Perception

Gary P. Misson[1,2], Stephen J. Anderson[1], Richard A. Armstrong[1], Mark Gillett[2], and David Reynolds[2]

[1] School of Optometry, School of Life & Health Sciences, Aston University, Birmingham, UK
[2] Department of Ophthalmology, South Warwickshire NHS Foundation Trust, Warwick, UK

Correspondence: Gary P. Misson, School of Optometry, School of Life & Health Sciences, Aston University, Birmingham B4 7ET, UK. e-mail: g.misson@aston.ac.uk

Received: July 8, 2020
Accepted: September 29, 2020
Published: October 28, 2020

Keywords: vision testing; macular pigment; vision; visual dysfunction; light polarization

Citation: Misson GP, Anderson SJ, Armstrong RA, Gillett M, Reynolds D. The clinical application of polarization pattern perception. Trans Vis Sci Tech. 2020;9(11):31, https://doi.org/10.1167/tvst.9.11.31

Purpose: Determine the repeatability of and optimum stimulus parameters for testing polarization pattern perception in a real-world clinical population, and assess the ability of polarization perception to distinguish normal from abnormal eyes.

Methods: Polarization perception was evaluated in staff and patients attending ophthalmology clinics at Warwick Hospital, UK. A series of visual stimuli were presented in pseudorandom order using a liquid-crystal-display–based polarization pattern generator. Stimuli included geometric patterns, gratings, checkerboards, and optotypes. Participants had one or both eyes diagnosed as normal or abnormal following ophthalmic examination, optical coherence tomography, and measures of visual acuity. Measurement scores were assigned to the eye(s) of each participant depending on the total number of stimuli perceived or identified.

Results: Stimuli covered the range of spatial scales resolvable within polarization perception by normal and abnormal eyes. Different stimuli had different saliencies. For each stimulus type, polarization perception in the abnormal group was significantly reduced compared with normal eyes ($P < 0.001$). Relative stimulus salience was broadly similar for normal-eye and abnormal-eye viewing groups, being greatest for radially symmetric patterns and least for optotypes. Checkerboard pattern salience had an inverse logarithmic relationship with check fundamental spatial frequency. A devised metric covering the dynamic range of polarization perception was repeatable, and the score derived from the metric was reduced in the abnormal group compared with the normal group ($P < 0.001$).

Conclusions: Clinically useful metrics of polarization perception distinguish between normal and abnormal eyes.

Translational Relevance: Perception of spatial patterns formed of non-uniform polarization fields has potential as a quantitative clinical diagnostic measurement.

Introduction

A large part of useful human vision is dependent on the fovea, an area of specialized high-acuity retina where lesions as small as 1.5 mm in diameter can render an individual legally blind. Early diagnosis of sight-threatening conditions that affect the fovea, such as age-related macular degeneration and diabetic eye disease, is essential for prompt treatment to prevent blindness. This study investigates the clinical diagnostic potential of our ability to detect polarization-modulated patterns, a recently described human visual phenomenon that is wholly dependent on intact foveal structure and function.

Amplitude, wavelength, and polarization are all fundamental wave properties of light. The most familiar type of polarization is linear polarization, where the electric field vector of all rays in a beam of light are constrained to vibrate in a single plane.

Many invertebrates have highly developed senses of polarization that are used variously for navigation, habitat selection, and communication.[1] Although amplitude and wavelength are perceived by humans as brightness and color, respectively, there are no familiar sensory correlates of polarization. However, under

specific conditions of illumination with a uniform field of blue linearly polarized light, a faint hourglass-shaped pattern, referred to as Haidinger's brushes (HB), can be perceived oriented perpendicular to the axis of polarization.[2] The percept fades after several seconds due to the Troxler phenomenon but can be made to persist by temporal modulation of the axis of polarization (e.g., rotation).

Polarization perception in humans is not limited to Haidinger's brushes. Non-uniform polarization-modulated fields of light yield percepts that can be made to vary in spatial complexity from simple one-dimensional patterns to complex optotypes.[3–5] This ability has been described as polarization pattern perception (PPP).[4]

Psychophysical investigations of PPP have demonstrated a remarkable ability of the human visual system to detect patterns modulated by as little as 5° of linear polarization axis orientation[5] and degrees of polarization down to less than 30%.[4,6] This ability matches that of some invertebrates and is currently thought to be unique among vertebrates. HB and PPP are manifestations of the same mechanism that requires an intact fovea and macular pigment.[5,7–9]

The human retina is structurally and functionally heterogeneous. The most sensitive part of the retina derives its name (macula lutea, "yellow spot") from the yellow plant-derived xanthophyll pigments present particularly at the fovea—the most central, 1.5-mm-diameter part of the macula aligned with the visual axis and possessing the greatest visual acuity. Specialized anatomical features of the fovea facilitating high visual acuity include modified densely packed photoreceptor outer segments, an absence of blood vessels, elongated radially displaced photoreceptor inner segments, and axons and supporting cells (Müller cells) comprising the Henle fiber layer.[10]

Although the origins of HB and PPP have yet to be fully elaborated, there is a general consensus that both phenomena involve differential absorption of linear polarized light by orientated macular pigment molecules associated with a radially symmetric Henle fiber layer.[2] The pigmented Henle fiber layer forms an absorbing filter that generates a polarization-dependent luminance signal, which is captured by underlying polarization-insensitive photoreceptor outer segments. This mechanism of detecting polarization signals differs from that of invertebrates, which have structurally different photoreceptors that are intrinsically polarization sensitive.[1]

Knowledge of the relationship between macular structure and the perception of HB spurred early attempts to use this phenomenon in the clinical assessment of macular function in pathological states.[11–13]

As a visual stimulus, the coarse spatial structure of HB has the advantage of being little affected by refractive error and media opacities,[7,12] qualities that also make the phenomenon potentially suitable as a prognostic indicator for cataract surgery. However, the coarse structure and transient nature of the HB percept necessarily impedes its clinical use in three ways. First, the short-lived, low-contrast static "brushes" are relatively difficult to perceive and demand an alert observer. Second, the low-spatial-frequency brush structure does not easily lend itself to a robust quantification of mild to moderate macular dysfunction. Third, the phenomenon is relatively non-specific with respect to its ability to differentiate among ocular diagnoses.[13] As a consequence, Haidinger's brushes have not been routinely used to assess macular function in clinical practice.

Here, we take a different approach to investigate the clinical utility of human polarization sensitivity by employing polarization-modulated pattern stimuli. Identifiable across a range of contrasts and scales, polarization patterns can be resolved with an acuity down to at least 0.3 logMAR[4] and, as noted above, are quantifiable in terms of both angle and degree of polarization. Furthermore, polarization-modulated patterns enable the generation of a wide variety of stimuli, potentially allowing for a detailed quantitative assessment of macular integrity.

This study first defines a set of robust polarization-modulated pattern stimuli that can be used in a clinical setting. The stimuli, detailed here and in the Supplementary Material, were used to investigate the differences in responses between visually normal and abnormal clinical populations.

Materials and Methods

All measurements were undertaken at the Machen Eye Unit of Warwick Hospital, South Warwickshire NHS Foundation Trust, Warwick, UK, between November 2017 and April 2019. The study adhered to the tenets of the Declaration of Helsinki and was approved by the National Health Service Health Research Authority (IRAS project ID 224715) following Research Ethics Committee approval (REC reference 17/WA/0180). All participants gave informed consent after explanation of the study.

Participant Characteristics

Participants were recruited from staff and patients at the Machen Eye Unit, Warwick Hospital (Table 1),

Table 1. Participant Summary Data

	Participants			Viewing Groups	
	All ($n = 334$)	Normal ($n = 90$)	Patients ($n = 244$)	Normal Eyes ($n = 126$)	Abnormal Eyes ($n = 452$)
Sex (*n*)					
Male	137	31	106	43	200
Female	197	59	138	83	252
Eye (*n*)					
Right	334	90	216	66	223
Left	334	90	221	60	229
Age (y)					
Mean	68.1	55.2	72.1	57.8	72.8
SD	15.1	15.3	12.6	15.3	12.2
Maximum	93.9	86.4	93.9	88.5	93.9
Minimum	18.0	18.0	20.8	18.0	20.8

and included individuals with both eyes normal (normal participants, $n = 90$) and those with eye pathology in one or both eyes (patients, $n = 244$). Data for the normal-eye viewing group (normal group, $n = 126$) used in the analyses included data from one eye (chosen at random) from the normal participants plus the clinically normal eye of patients with unioocular pathology (e.g., posterior vitreous detachment, corneal scar, ocular trauma). Data for the abnormal-eye viewing group (abnormal group, $n = 452$) included data from one or both abnormal eyes of patients. Although we recognize that the use of both eyes from single individuals might introduce bias, we considered that the asymmetry of similar pathology and different pathology in paired eyes justified our approach, at least for the present study. The diagnostic categories of the viewing eyes of the participants are given in Supplementary Table S1. For the repeatability data, a subset of normal participants ($n = 34$) was tested twice.

Baseline measures of best-corrected logMAR visual acuity were recorded for all individuals. Distance refractive error was noted, and an ophthalmic assessment was performed comprised of slit-lamp examination, fundoscopy, and optical coherence tomography (OCT). The allocation of individuals to diagnostic categories was based on clinical examination and OCT.

Polarization Pattern Perception Testing

Polarization-modulated patterned visual stimuli were generated using a 27-inch, thin-film transistor, liquid-crystal display (Asus VS278H; ASUSTeK Computer, Inc., Taiwan, provided by Optical Diagnostics Ltd., Coventry, UK) from which the front polarizer had been removed to produce a delaminated liquid-crystal display (dLCD). The resolution of the display was 1920 × 1080 pixels. Full details of this display modification process are described elsewhere.[3–5,14] Filters positioned within the dLCD allowed for a uniform luminosity blue field with a peak wavelength of 460 nm, corresponding to the peak sensitivity of polarization pattern perception.[4] The dLCD enables the presentation of a spatial image that is modulated by angle of polarization but with constant luminance across the screen. The specific polarization angle (**E** vector) orientation emitted by the dLCD depends on the grayscale values used to define the foreground and background of the displayed spatial image.

The viewable screen area of the device used in this study subtended a visual angle of 11° × 6.5° at an observation distance of 3 m. Luminous output, measured with a Minolta photometer (Chroma Meter CS100-A; Konica Minolta, Tokyo, Japan), was constant at 8.0 cd·m^{-2} across the entire screen area for all polarization states (image grayscale values). Polarimetry was performed using standard methods[5,14] at a working wavelength of 460 nm. Two polarization outputs were measured, corresponding to the foreground of the image (acuity letter or component of the pattern stimulus corresponding to a grayscale of 000, or black) and the background of the image (component of the pattern with a grayscale of 255, or white). The angles of polarization of the foreground and background, measured counterclockwise from horizontal, were 54° and 147°, respectively (i.e., there was a foreground–background difference in angle of polarization of 87°). The degree of linear polarization for both the foreground and background was 0.94, with

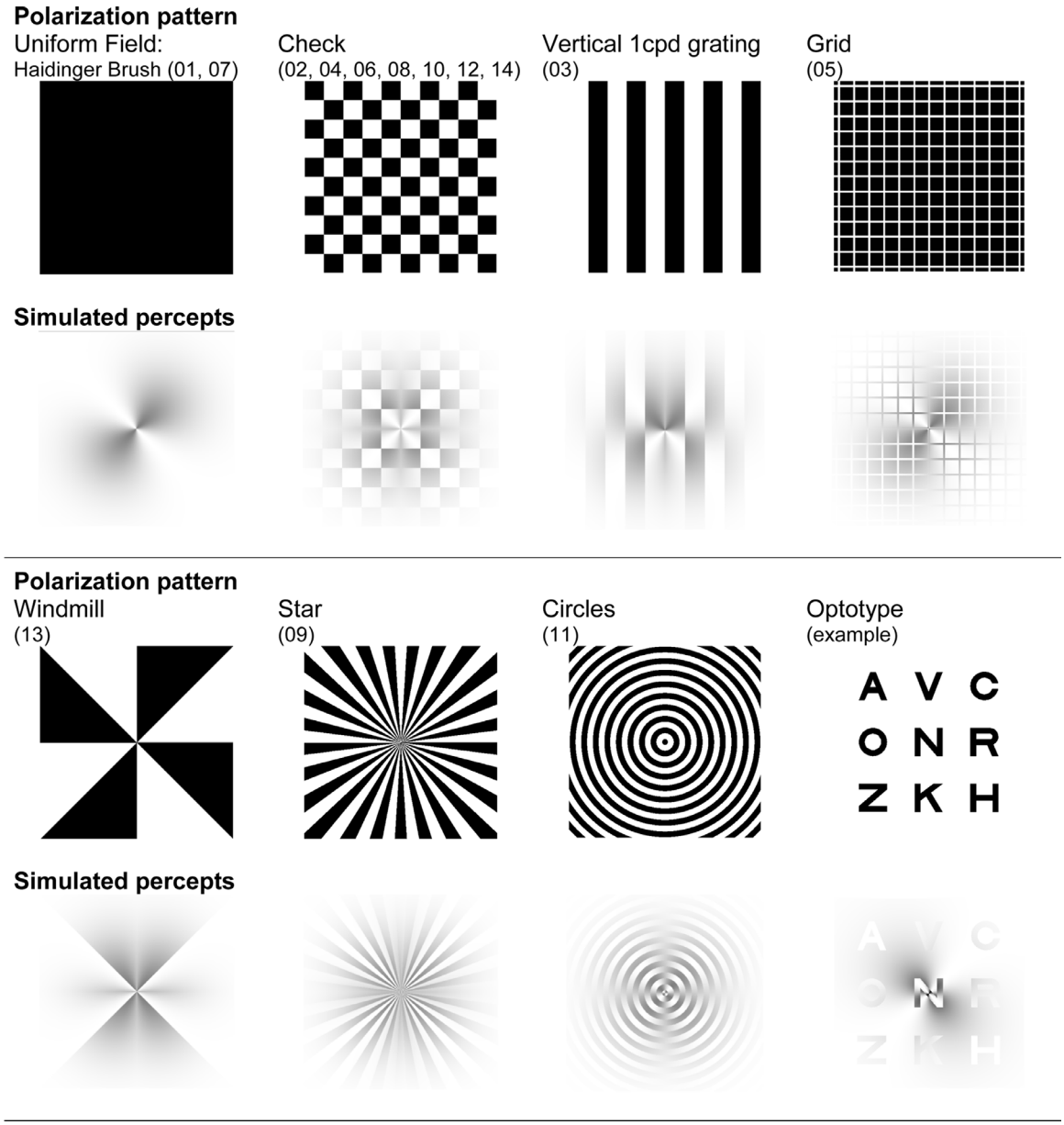

Figure 1. Polarization pattern stimuli (first and third rows) with simulated percepts (second and fourth rows). Simulations were generated assuming foveal fixation at the geometric center of each stimulus. The optotype example and simulated percept (bottom right) are typical of the logMAR 1.0 optotype stimuli used in the study. Note that three rows are given here as an example, although single lines of five letters were presented in the test protocol. Detailed explanations of the figures and simulations are given in the Supplementary Material.

minimal ellipticity (the ratio of the minor to the major axes of the polarization ellipse was 0.08).

A full psychometric evaluation of polarization pattern perception[5,6] is not feasible or appropriate in a clinical setting, principally for reasons of test duration, participant fatigue, and participant comprehension. Here, utilizing the psychophysical measures of sensitivity reported by Misson and Anderson,[5] we developed a robust, rapid, and easily performed protocol for the assessment of PPP on a clinical population. The full protocol was comprised of a series of 14 spatial patterns and logMAR-graded Sloan optotypes.[15] The stimuli, together with their simulated foveal fixation percepts, are shown in Figure 1 and explained in detail in the Supplementary Material and Supplementary Movie S1.

Ametropic participants were corrected for the working distance of the test using optically anisotropic (stress-free) trial lenses supported in a trial frame. All testing was monocular, with each eye of a

participant assessed in turn. Patterns were displayed on the dLCD in pseudorandom order as a PowerPoint (Microsoft, Redmond, WA) slide presentation, with each image slide containing a single stimulus pattern. Image presentation was controlled by the operator, with the viewing time for each slide limited to a maximum of 30 seconds. Participants were required to observe the center of the screen for each image presentation. Head stabilization was not employed.

Two response criteria were used. First, participants were asked if they could see a patterned image or simply a blank blue screen, and a positive response was recorded as pattern perception. Second, participants giving a positive pattern perception response were asked whether they could describe the pattern, and a positive response for pattern identification was recorded if the observer was able to describe the general appearance of the displayed image. Accepted terms included vertical bars, concentric rings, checks or checkerboard, star or starburst, and windmill or triangles. Letter identification was required for the optotype images.

Testing was performed by one of two trained ophthalmic technicians, neither of whom was aware of the participants' diagnoses. Typical runtimes for the full series of slides were between 10 and 15 minutes per eye. Before testing and data recording, the technician explained the task and the expected appearance of the stimuli according to a set preamble.

Statistical Methods

Conventional methods for analysis of parametric data were used. A non-parametric approach was adopted for quantized/discontinuous score data. The following were used where appropriate: Kruskal–Wallace test of ranks and the Mann–Whitney U test for comparison of two independent samples and χ^2.

The Cochran–Mantel–Haenszel Test was used to test multiple 2×2 contingency tables. In the case of the present study, the test was used to determine whether there was a significant difference between the odds ratios of normal-eye and abnormal-eye viewing across the different stimuli. Woolf's test was then applied to determine the heterogeneity of the odds ratios for individual stimuli within a set.

Scatterplots were used to demonstrate repeatability of measurements, as were Bland–Altman plots. Although the latter are intended for parametric data, they provide a useful indication of repeatability. For correlation of visual acuity and polarization scores, deviations of the data from a bivariate normal model were insufficient to reject the use of Pearson product–moment correlation coefficients.

Results

Stimulus-Specific Responses

For the criteria of pattern perception and pattern identification, data were categorized into responses for patterns or optotypes.

Normal-Eye Viewing

For the 126 individuals in the normal-eye viewing group, 119 (94.4%) perceived one or more of the 14 geometric stimuli, with 111 (88.1%) individuals being able to identify one or more of the geometric stimuli.

The geometric stimuli were graded in salience with respect to the criteria of pattern perception and pattern identification (Fig. 2a, Table 2). The large pattern-reversing checks, radial (star), windmill, concentric circle, and alternating HB patterns had a perception rate of ≥84%, which contrasted with a perception rate of 48% for the static HB. The remaining geometric patterns were perceived between 30% and 80% of the time. Note that no pattern type was identified as often as it was perceived (i.e., although some individuals perceived the presence of a pattern, they were unable to correctly identify it). The concentric circles and radial star pattern were the most readily named, each with an identification rate of approximately 75%.

The optotype stimuli were also graded in salience for the criterion of letter identification (Fig. 2b), for each logMAR value and within each logMAR banding. Compared with geometric patterns, optotypes were less well identified. Within each logMAR banding, the most readily identified letter was Z, with the 1.2-logMAR optotype being identified 41% of the time with normal-eye viewing.

For geometric patterns, a measure of how well a stimulus can be identified can be obtained by plotting the difference in positive responses for perception and identification (PI difference) against the absolute number of positive identifications for each pattern (Fig. 3): the lower the PI value, the greater the number of positive identifications. Note that the graded pattern-dependent descent in the frequencies of identification follows a different order from that identified above. The radial static stimuli (red square symbols for windmill, circles, and star; #13, #11, and #09) were identified by a greater number of individuals compared with other stimuli, and with a lower than mean PI difference (i.e., more easily identified). The uniform field stimuli (green squares for alternating and static HB; #01 and #07) had the highest PI differences (i.e., were least easily identified). Values for the

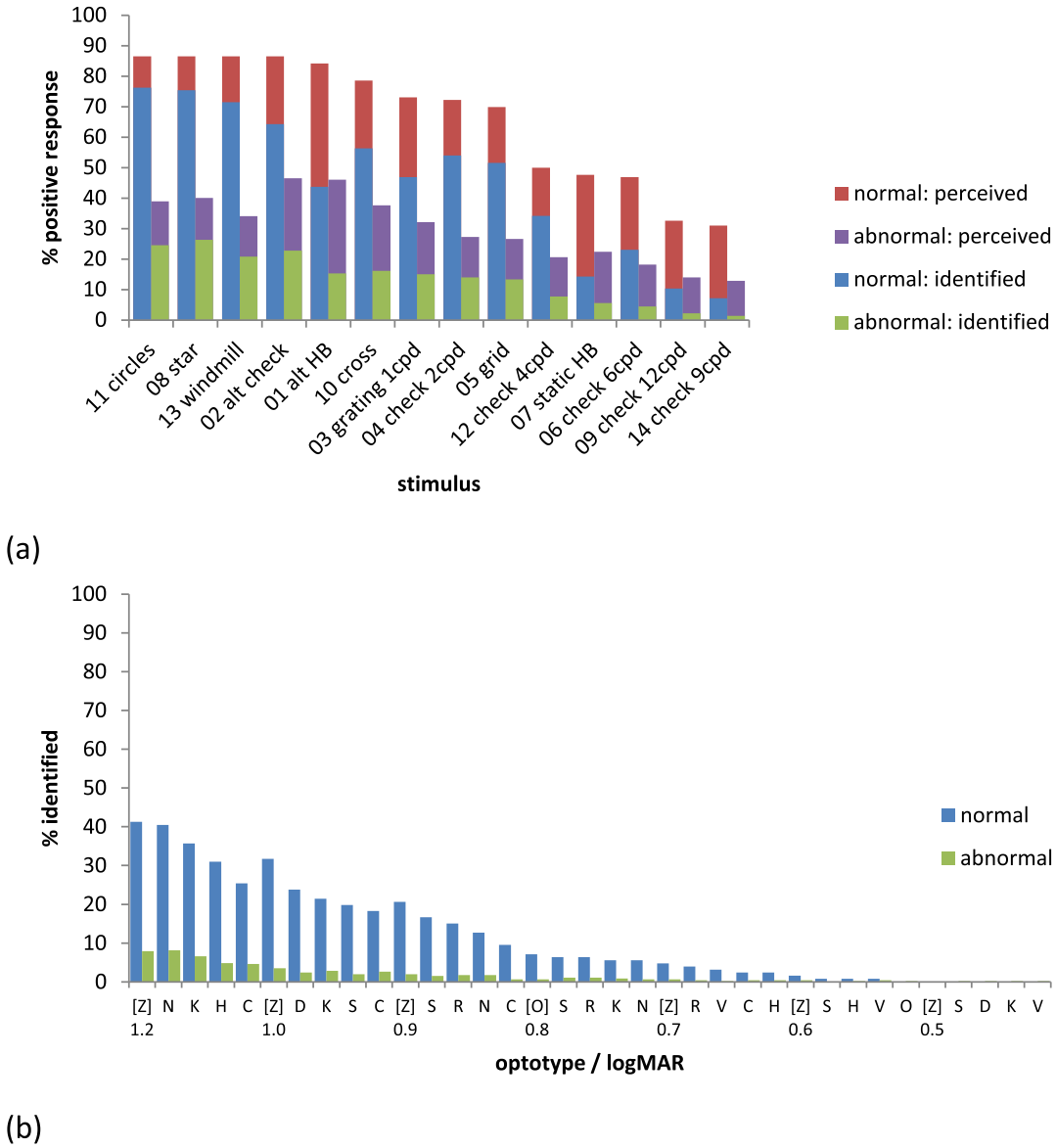

Figure 2. Proportions of stimuli perceived/identified for normal- and abnormal-eye viewing. (a) Pattern stimuli. *Blue/red columns* are for normal-eye viewing; *green/purple columns* are for abnormal-eye viewing. The height of the *blue/green columns* shows the percentage of each stimulus identified; the height of the *red/purple columns* shows the percentage of each stimulus perceived. (b) Percentage of optotypes identified. The abscissa shows the optotypes in groups of five, with corresponding logMAR values of 1.2, 1.0, 0.9, 0.8, 0.7, 0.6, and 0.5. Square brackets demarcate the boundary of each logMAR banding.

rectilinear stimuli (checkerboard, grid, and grating) mostly fell within the 95% confidence interval (CI) of the PI difference mean (Fig. 3), indicating that this pattern type was consistently identified.

A further finding for the checkerboard patterns was a decrease in both perception and identification frequency with the logarithm of the check size fundamental frequency (Fig. 4).

Abnormal-Eye Viewing

With abnormal-eye viewing, 61% (275 of 452 abnormal eyes) of individuals perceived at least one pattern, whereas 41% (187 abnormal eyes) identified at least one pattern (Fig. 2a). Optotypes were poorly perceived with abnormal-eye viewing, with less than 10% of individuals identifying one or more optotypes (Fig. 2b).

For most stimuli, the general trend of pattern perception and identification was similar to normal-eye viewing (Fig. 2, Table 2). The exception was the alternating HB stimulus, which, with abnormal-eye viewing, was perceived with the same frequency as the alternating checkerboard pattern (46%), but both of these patterns were relatively more salient

Table 2. Pattern Stimulus Responses to Pattern Perceived Criterion Given As Number of Positive Responses (*F*) and Percentage for Normal- and Abnormal-Eye Viewing, Ranked by Decreasing Odds Ratio

	Normal ($n = 126$)			Abnormal ($n = 452$)			Odds	Rank
Stimulus	*F*	%	Rank	*F*	%	Rank	Ratio	Odds
Windmill, #13	109	86.5	1	154	34.1	6	12.41	1
Circles, #11	109	86.5	1	176	38.9	4	10.05	2
Star, #08	109	86.5	1	181	40.0	3	9.60	3
Alternating check, #02	109	86.5	1	210	46.5	1	7.39	4
Check (2 cpd), #04	91	72.2	8	123	27.2	8	6.95	5
Grid, #05	88	69.8	9	120	26.5	9	6.41	6
Alternating HB, #01	106	84.1	5	208	46.0	2	6.22	7
Cross, #10	99	78.6	6	170	37.6	5	6.08	8
Grating (1 cpd), #03	92	73.0	7	145	32.1	7	5.73	9
Check (6 cpd), #06	59	46.8	12	82	18.1	12	3.97	10
Check (4 cpd), #12	63	50.0	10	93	20.6	11	3.86	11
Static HB, #07	60	47.6	11	101	22.3	10	3.16	12
Check (9 cpd), #14	39	31.0	14	58	12.8	14	3.05	13
Check (12 cpd), #09	41	32.5	13	63	13.9	13	2.98	14

	Cochran–Mantel–Haenszel Test	Woolf Test
M	848.6	45.1
P	<0.001	<0.001
Odds ratio	5.6	–
Lower 95% CI	5.0	–
Upper 95% CI	6.4	–

The criterion was stimulus perceived (seen/identified) versus not perceived.

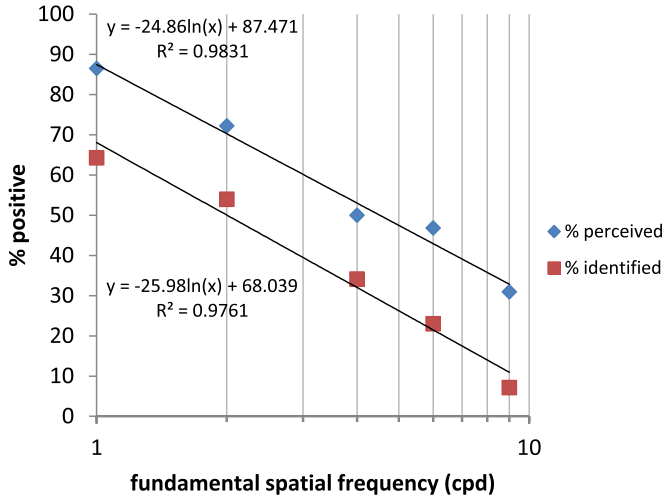

Figure 3. Percentage of positive responses for pattern perception and pattern identification of checkerboard images for normal-eye viewing, plotted against the log of the checkerboard fundamental spatial frequency (range, 1–9 cpd). The *solid line* through each dataset is the least-squares best fit, with regression equations shown.

than the stimuli with radial symmetry (circle star and windmill).

The ability to perceive and identify each pattern or optotype stimulus was significantly reduced with abnormal-eye viewing compared with normal-eye viewing (Cochran–Mantel–Haenszel test for multiple contingency tables; see pattern perception data in Table 2). For pattern identification, $M = 903.3$, odds ratio = 6.5, and $P < 0.001$; for optotype identification, $M = 960.5$, odds ratio = 8.7, and $P < 0.001$. An odds ratio of 5.6 (95% CI, 5.0–6.4) (Table 2) indicates that, for the pattern stimuli, the ratio of positive to negative results for pattern perception was 5.6 times greater for normal-eye viewing compared with abnormal-eye viewing ($P < 0.001$). The individual odds ratios for each stimulus indicate which patterns are likely to better differentiate abnormal from normal (Table 2). The radially symmetric stimuli (windmill, circles, and star) had high individual odds ratios (>9), far exceeding the upper 95% confidence level for the overall odds ratio of the stimulus set (6.4).

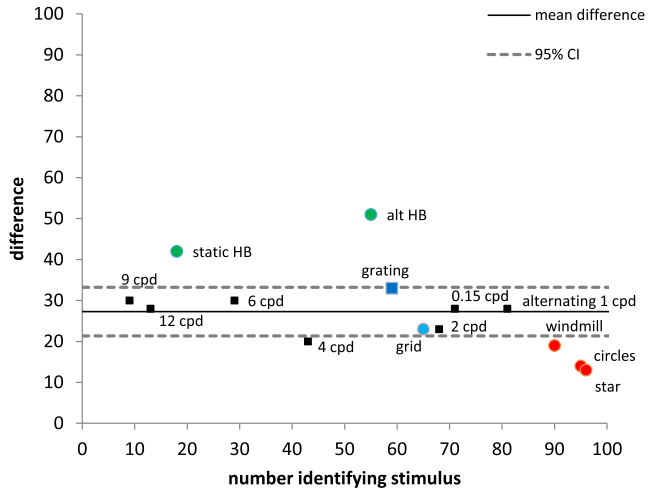

Figure 4. Difference in positive responses for perception and identification for normal-eye viewing (PI difference), plotted against the absolute number of positive identifications for each pattern. Different color squares are used for each stimulus type: checkerboards (*black*), grating (*dark blue*), grid (*light blue*), Haidinger's brushes (*green*), and windmill, circles, or radial pattern (*orange*). Mean difference (*black continuous line*) and 95% CIs (*dotted lines*) are shown. The salience of most patterns exhibited consistent degrees of variation within the confidence limits, apart from the Haidinger's brushes stimuli (higher PI difference) and the radial-patterned stimuli (lower PI difference).

Individual Responses to Polarization Pattern Stimuli: Normal Versus Abnormal

The preceding section was concerned with the number of participants responding to a particular stimulus. This section investigates the overall stimulus response of normal-eye compared with abnormal-eye viewing.

Metrics of Polarization Perception and Their Repeatability

A simple single metric is required for quantifying the ability of individual observers to see polarization pattern-modulated stimuli. The simplest parameters are the number of patterns perceived (Pp) or identified (Pi) and the number of optotypes identified (Oi). The previous section showed that there is effectively a graded progression in salience from the higher salience pattern stimuli to the optotype responses. Here, we combine these two sets of measurements in a single metric to increase the dynamic range of responses. Two combined metrics were considered: pattern identification + optotype identification (Pi+Oi) and pattern perception + optotype identification (Pp+Oi). Acknowledging that the latter involves mixing psychophysical criteria, its clinical utility will be investigated further.

Repeatability of Pi+Oi and Pp+Oi

A cohort of normal participants ($n = 34$) had repeat measurements of PPP after an interval ranging from 1 day to 18 months. Figure 5 shows the test–retest data for right-eye viewing for the criteria of identification of both geometric patterns and optotypes (Pi+Oi) and for the combined criteria of perception of the pattern (i.e., seeing a pattern but not necessarily being able to identify it) and identification of optotype (Pp+Oi). The solid diagonal lines in Figures 5a and 5c show the lines of equivalence, and the broken lines show the least-squares best fit to the data.

There was no significant difference found between normal right and normal left eye datasets (Wilcoxon signed-rank test for paired samples; Pi+Oi, $P = 0.24$; Pp+Oi, $P = 0.49$).

The repeatability and individual pattern response data from normal-eye and abnormal-eye groups indicate that both combined criteria Pi+Oi and Pp+Oi were repeatable and that both had a sufficient dynamic range to cover the responses of normal and abnormal viewing eyes.

Participant-Specific Responses: Normal Versus Abnormal

Percentage frequency histograms for various response criteria are shown in Figure 6 for both the normal and abnormal groups. For all criteria (Oi, Pi, Pp, Pi+Oi, and Pp+Oi), the differences between normal and abnormal groups were statistically significant (χ^2, $P < 0.001$).

The frequency peaks show the greatest separation of Pp scores (Fig. 6d), which, when combined with the optotype identified criterion (Fig. 6a), provided a metric that both discriminated abnormal from normal and covered the widest range of values (Fig. 6e). The Pp+Oi responses of abnormal versus normal groups were significantly different (Mann–Whitney $U = 9537.5$, $P < 0.001$). The combined Pp+Oi metric will therefore be used in further analyses.

Effect of Age, Gender, and Laterality on Normal Pp+Oi Scores

The effect of age, gender, and laterality on Pp+Oi was determined for the normal group. Linear regression analysis of Pp+Oi against age, although statistically significant, was weak (Pp+Oi = 18.540 – [0.114 × age]; $r = 0.210$; $P = 0.031$; $r^2 = 0.044$). We noted less variation in values for individuals over the age of 55 years and took this age as an arbitrary boundary. There was no statistically significant difference (Mann–Whitney $U = 1099$; $P = 0.08$) in the median Pp+Oi scores for individuals < 55 years ($n = 47$; median

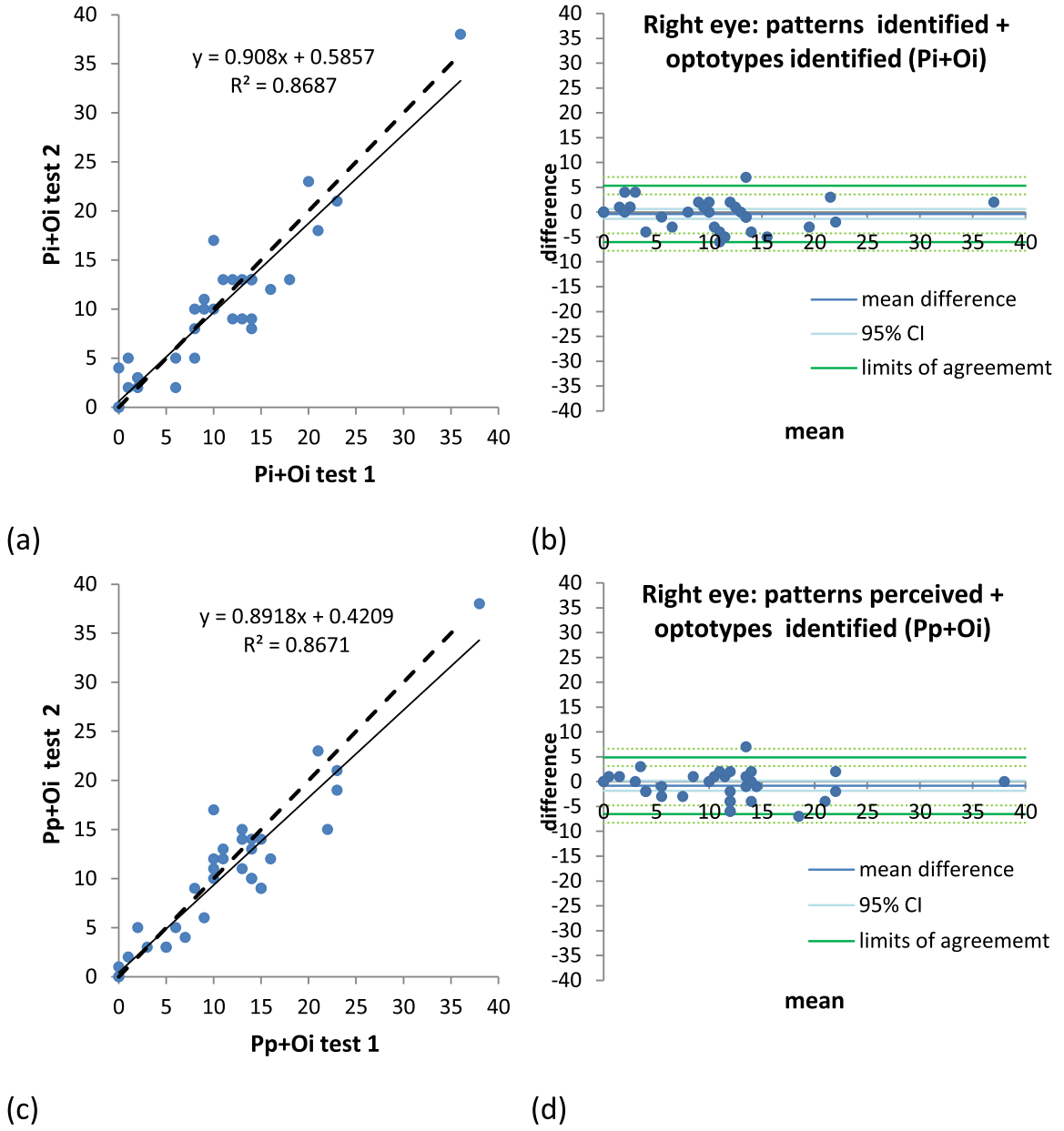

Figure 5. Repeatability of scoring metrics Pi+Oi and Pp+Oi for normal right eyes ($n = 34$). (a) Scatterplot of test–retest Pi+Oi data, showing line of equivalence (*dashed line*) and best-fit regression function (*continuous line*, with regression equation). (b) Bland–Altman plot of test–retest difference versus test mean value. Bias = –0.4; limits of agreement, ±5.7 points. For scoring metric Pp+Oi, bias = −0.8, limits of agreement = ±5.7 points.

Pp+Oi = 12) compared with those ≥ 55 years ($n = 59$; median Pp+Oi = 9). Furthermore, there was no significant effect on Pp+Oi of either gender (Mann–Whitney $U = 1567.5$; $P = 0.13$; female, $n = 83$, median Pp+Oi = 12; male, $n = 43$, median Pp+Oi = 11) or laterality (Mann–Whitney $U = 1586.5$; $P = 0.06$; left eye, $n = 60$, median Pp+Oi = 10; right eye, $n = 66$, median Pp+Oi = 13).

No significant difference (Mann–Whitney $U = 1497$; $P = 0.51$) was found when comparing Pp+Oi scores of the normal subject component ($n = 90$; median score = 13) of the normal-eye viewing group with the scores from normal eyes of the patient component ($n = 36$; median score = 14). This supports the use of the composite normal-eye viewing dataset.

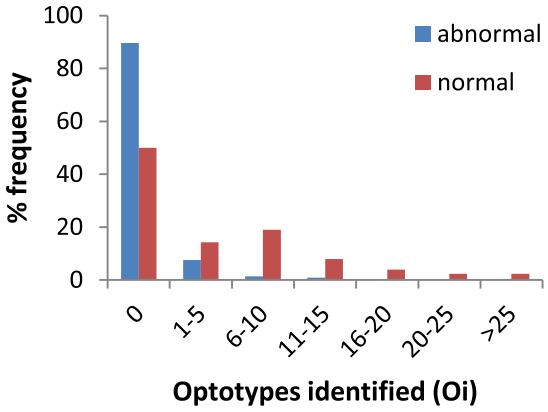

(a) Optotype identified (Oi)

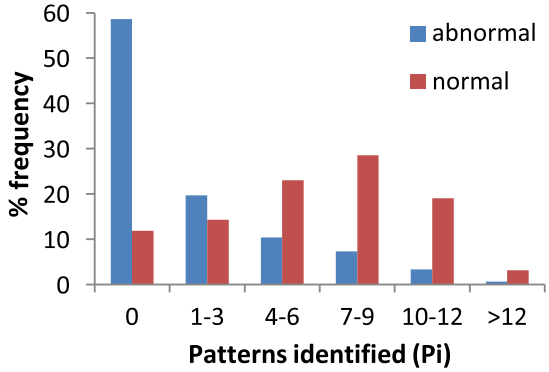

(b) Pattern identified (Pi)

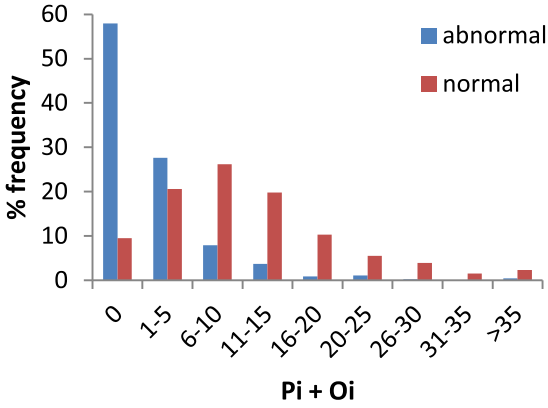

(c) Combined pattern and optotypes identified (Pi+Oi)

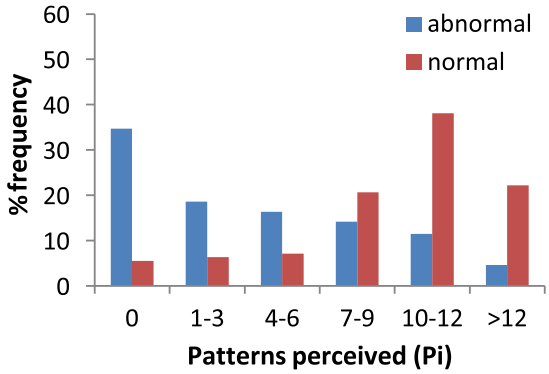

(d) Pattern perceived (Pp)

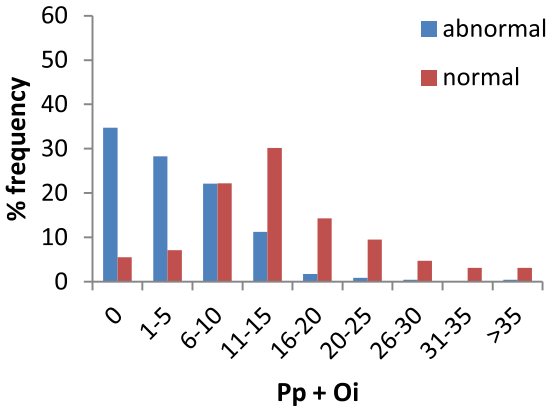

(e) Combined pattern perceived and optotypes identified (Pp+Oi)

Figure 6. Frequency histograms for different response criteria for normal-eye (*blue*) and abnormal-eye (*brown*) viewing. See text for definition of response criteria.

Pp+Oi Scores and Visual Acuity

The logMAR visual acuities of the normal (mean, 0.04; SD = 0.15) compared to abnormal (mean, 0.36; SD = 0.51) groups were significantly different (t = 5.26; $P < 0.001$). A weak correlation between Pp+Oi scores and logMAR visual acuity was found in both the normal (Pearson correlation $r = –0.25$; $P = 0.02$) and abnormal ($r = –0.13$; $P = 0.006$) groups.

Discussion

The principal aim of this study was to determine whether the perception of patterned polarized light could be used to differentiate between individuals with normal eyes and individuals with abnormal eyes. The definition of abnormal is taken here as a heterogeneous selection of conditions (see Supplementary Table S1) that include sight-threatening pathology and non-sight-threatening conditions such as pseudophakia.

As the novelty of our approach precluded the use of pre-existing clinical data in the development of appropriate test patterns, the design of the stimuli was largely based on the known perceptual responses to both equivalent luminance stimuli and polarization stimuli, as well as the radially symmetric geometry of human polarization perception.[3,5] The developed stimuli were intended to give a graded and quantifiable measure of polarization perception over a suitable response range for naïve individuals with either normal or abnormal eyes.

Two response criteria were investigated: the ability to distinguish an image from a blank background (pattern perception) and the ability to identify the geometry of the image or to name an optotype (pattern/optotype identification). Both criteria were demonstrated to be appropriate for the ranges of normal-eye and abnormal-eye responses (Fig. 2). The responses to different patterned and optotype stimuli presented in polarized light formed a graded profile for normal and abnormal groups, with a significant difference between the groups.

The most readily perceived and identified stimuli were those with either a defined radial structure (concentric circles, radial, and windmill images) or a dynamic low-spatial-frequency component (large pattern-reversing checks and alternating Haidinger's brushes) (Figs. 2a, 4; Table 2; Supplementary Movie S1). The most salient optotype (Z) was comprised of both rectilinear and oblique (i.e., radial) components. An optimal pattern stimulus for polarization perception, rather than a checkerboard as previously assumed, might therefore be composed of elements with higher orders or radial symmetry. It is known that the macular structures underlying the mechanism of human polarization perception are radially symmetric.[2,16] Any link between polarization stimulus symmetry preference and the symmetry of macular architecture requires further investigation, particularly because macular disease such as age-related macular degeneration disrupts the macular architecture.

The rectilinear stimuli were most consistently perceived over a range of identification frequencies (i.e., deviated least from the mean PI difference, as shown in Fig. 4). Furthermore, the suitability of the checkerboard stimuli as a psychophysical measure of polarization sensitivity in a clinical setting is supported by the demonstration of an inverse log-linear relationship between checkerboard stimulus salience and the fundamental spatial frequency of each stimulus (Fig. 3). This relationship breaks down for the smallest check size employed (12 cpd), which approaches the limit of spatial resolution for polarization patterns.[4]

Six percent of the normal group were unable to perceive any of the stimuli. Possible non-pathological reasons for this include depolarization by ocular media, variability in cognitive ability, and known physiological variability in macular pigment concentration[17] or foveal structure.[10] Undiagnosed pathology is also a potential cause and, as with demonstrable pathology, could disrupt polarization perception at three levels: (1) depolarization or anomalous absorption by abnormal ocular media, (2) failure of differential absorption by abnormal inner foveal layers, or (3) photoreceptor malfunction. An hypothesis under investigation is that disorders of the inner retina with intact photoreceptors, such as early diabetic macular edema and vitreomacular interface pathology (e.g., epiretinal membranes), might preferentially affect polarization sensitivity before visual acuity.

The difference between normal and abnormal populations with respect to the responses to individual stimuli is clear from Figure 2a and Table 2. Importantly, from the overall odds ratio result, the overall ratio of stimuli perceived to not perceived for normal eyes was 5.6 times greater than that for abnormal eyes. The individual odds ratios for pattern stimuli were heterogeneous ($P < 0.001$, Woolf test) (Table 2). The odds ratios for the radial patterns (windmill, circles, and star) exceeded the upper confidence interval for the overall odds ratio. These patterns are therefore not only more salient for normally sighted individuals but also best suited for differentiating normal-eye from abnormal-eye groups.

The optotype stimuli were generally the most difficult to perceive, even by individuals with normal vision. This finding supports a previous report that, with

polarization patterns, the Landoldt-C optotype has less salience than grating stimuli.[5] Likely reasons for this difference include the spatial complexity of optotype images compared with geometric patterns and the localized nature of optotypes being more dependent on scanning eye movements for the detection of edge boundaries. Polarization perception is foveal, being limited to the central 5° of visual field; therefore, images falling outside this area are not perceived. Although the sole use of optotype stimuli may be of limited value in a clinical setting, their use in combination with other geometric patterns ensures coverage of the full dynamic range of polarization pattern perception (Fig. 2).

The pattern perception and optotype identification metric (Pp+Oi) and the pattern and optotype identification metric (Pi+Oi) were both repeatable (Fig. 5). The combined Pp+Oi metric was chosen as the optimum for further clinical investigation because the normal and abnormal response distributions showed the greatest separation of peaks and approximately equal maxima (compare Fig. 6e with Fig. 6c). Moreover, this metric was independent of gender and age for our normal group.

The weak correlation of Pp+Oi with visual acuity in both normal and abnormal groups accounts for 6% or less of the variance (normal $r^2 = 0.06$; abnormal $r^2 = 0.02$). We conclude that the polarization metric measures a functional parameter distinct from that measured by visual acuity.

Patterned polarization perception and the phenomenon of Haidinger's brushes are both dependent on intact foveal function and architecture. Despite being promoted over several decades as a possible clinical test of macular function,[7,9,11–13] the classic Haidinger's brush phenomenon has never gained acceptance in routine clinical practice. Unlike Haidinger's brushes, however, polarization pattern perception requires the delineation of structured edges. This single attribute facilitates a novel approach to using polarization perception as a clinical tool, with the potential advantages that it is readily quantifiable and can be assessed with inexpensive, highly portable, solid-state liquid-crystal-based technology.

Acknowledgments

The authors thank the following: the staff of the Machen Eye Unit, South Warwickshire NHS Trust, particularly Alison Marriot (Departmental Manager), Sara Queen (Clinical Director), and Jo Williams (Head of Research); Mark Dunne, PhD (Aston University, UK), for support with statistical analyses; and Shelby E. Temple, PhD, for critical review of the manuscript.

GPM is the recipient of a grant from the European Society of Cataract and Refractive Surgeons.

GPM conceived of the study, built the equipment, and was project administrator; GPM and SJA designed the experiments and wrote the paper; MG and DR were responsible for data acquisition and database management; GPM, SJA, and RAA performed data analyses; SJA performed psychophysical analyses; and RAA, MG, and DR reviewed the paper.

Disclosure: **G.P. Misson,** None; **S.J. Anderson,** None; **R.A. Armstrong,** None; **M. Gillett,** None; **D. Reynolds,** None

References

1. Marshall NJ, Powell SB, Cronin TW, et al. Polarisation signals: a new currency for communication. *J Exp Biol*. 2019;222:1–16.
2. McGregor J, Temple SE, Horváth G. Human polarization sensitivity. In: Horváth G, ed. *Polarized Light and Polarization Vision in Animal Sciences*. Heidelberg: Springer; 2014:303–315.
3. Misson GP, Timmerman BH, Bryanston-Cross PJ. Human perception of visual stimuli modulated by direction of linear polarization. *Vision Res*. 2015;115:48–57.
4. Temple SE, McGregor JE, Miles C, et al. Perceiving polarization with the naked eye: characterization of human polarization sensitivity. *Proc Biol Sci*. 2015;282(1811):20150338.
5. Misson GP, Anderson SJ. The spectral, spatial and contrast sensitivity of human polarization pattern perception. *Sci Rep*. 2017;7:16571.
6. Misson GP, Temple SE, Anderson SJ. Computational simulation of human perception of spatially dependent patterns modulated by degree and angle of linear polarization. *J Opt Soc Am A Opt Image Sci Vis*. 2019;36(4):B65–B70.
7. Stanworth A, Naylor EJ. The measurement and clinical significance of the Haidinger effect. *Trans Ophthalmol Soc U K*. 1955;75:67–79.
8. Bone RA. The role of the macular pigment in the detection of polarized light. *Vision Res*. 1980;20(3):213–220.
9. Muller PL, Muller S, Gliem M, et al. Perception of Haidinger brushes in macular disease depends on macular pigment density and visual acuity. *Invest Ophthalmol Vis Sci*. 2016;57(3):1448–1456.

10. Provis JM, Dubis AM, Maddess T, Carroll J. Adaptation of the central retina for high acuity vision: cones, the fovea and the avascular zone. *Prog Retin Eye Res*. 2013;35:63–81.
11. Goldschmidt M. A new test for function of the macula lutea. *Arch Ophthal*. 1950;44(1):129–135.
12. Forster HW Jr. The clinical use of the Haidinger's brushes phenomenon. *Am J Ophthalmol*. 1954;38(5):661–665.
13. Sloan LL, Naquin HA. A quantitative test for determining the visibility of the Haidinger brushes: clinical applications. *Am J Ophthalmol*. 1955;40(3):393–406.
14. Foster JJ, Temple SE, How MJ, et al. Polarisation vision: overcoming challenges of working with a property of light we barely see. *Naturwissenschaften*. 2018;105(3–4):27.
15. Pelli DG, Robson JG, Wilkins AJ. The design of a new letter chart for measuring contrast sensitivity. *Clin Vision Sci*. 1988;2(3):187–199.
16. Misson GP, Temple SE, Anderson SJ. Polarization perception in humans: on the origin of and relationship between Maxwell's spot and Haidinger's brushes. *Sci Rep*. 2020;10(1):108.
17. Hammond JBR, Wooten BR, Snodderly DM. Individual variations in the spatial profile of human macular pigment. *J Opt Soc Am A Opt Image Sci Vis*. 1997;14(6):1187–1196.

Supplementary Material

Supplementary Movie S1. Animation of the kinetic polarization stimuli and their respective perceptual simulations for foveal fixation. Stimulus #01, alternating Haidinger's brushes; stimulus #02, pattern reversing (alternating) checkerboard.